PHYSICAL REVIEW B VOLUME 43, NUMBER 13 1 MAY 1991

Optical-phonon study of single crystals of various layered cuprates and related materials: Evidence of unique electron-phonon coupling in the CuO_2 plane

S. Tajima
Superconductivity Research Laboratory, ISTEC, Shinonome 1-10-13, Tokyo 135, Japan

T. Ido, S. Ishibashi, T. Itoh, and H. Eisaki
Department of Applied Physics, The University of Tokyo, Hongo 7-3-1, Tokyo 113, Japan

Y. Mizuo
Department of Physics, Tokai University, Kitakaname 1117, Hiratsuka 259-12, Japan

T. Arima
Department of Physics, The University of Tokyo, Hongo 7-3-1, Tokyo 113, Japan

H. Takagi and S. Uchida
Department of Applied Physics, The University of Tokyo, Hongo 7-3-1, Tokyo 113, Japan

(Received 11 July 1990; revised manuscript received 7 December 1990)

Optical-phonon spectra were investigated for single crystals of the parent materials of various cuprate superconductors and related materials. Comparing the spectra, all the observed phonons were unambiguously assigned. It was found that the main phonon modes in the CuO_2 plane, the Cu-O stretching and bending modes, exhibit completely different dependences of their frequency on the Cu-O bond distance $a/2$; that is, the former shows strong a dependence while the latter is relatively insensitive to a. From a quantitative analysis of the spectra, the highly covalent character of these layered cuprates was confirmed. The remarkable change of the stretching-mode frequency against a indicates a direct coupling of this phonon with the Cu-O charge-transfer electronic excitation.

I. INTRODUCTION

The treatment of high-T_c copper oxide as an ionic crystal has been attempted by several researchers. One of the typical studies was the calculation of the Madelung potential of the Cu and/or O site.[1] However, in discussing the behavior of the doped holes and electrons, the transfer energy or the orbital hybridization is an indispensable factor. The problem is how this factor is related to the ionic potential.

In general, for an experimental investigation of the electric field in a crystal, a useful method is the measurement of the optical-phonon spectrum, by which we can know how covalent or ionic the crystal is and how strongly the electronic system couples with a certain phonon. In the case of high-T_c copper oxides, the direct role of phonons in the superconductivity mechanism seems to be discolored because of their high-T_c value.[2] However, some evidences for electron-phonon coupling have been reported by neutron scattering measurements,[3] photoinduced absorption measurements,[4] Raman scattering measurements,[5] etc. Thus, the role of phonon in the electronic system is an unsettled problem for these cuprates.

On the other hand, it is well known that the two-dimensional CuO_2 network is a common structure in all of the high-T_c cuprates and it plays an essential role in realizing high T_c. Therefore, the bonding state in the CuO_2 plane is the most important target for the phonon study of these materials. In order to extract the phonons associated with Cu and O atom in the plane, it is necessary to assign the phonon mode for all of the observed phonon peaks in the spectra.

Concerning the phonon mode assignment, there were a hundred reports,[6] but they were controversial. One of the reasons for this confusing situation is the use of polycrystalline samples for such anisotropic materials. For the data of polycrystals, quantitative analysis (for example, Kramers-Kronig analysis and the oscillator fitting analysis) cannot be applied. Therefore, we can determine neither the oscillator strength nor even the phonon frequency when both frequencies of the phonons parallel and perpendicular to the c axis are close to each other and they form a single broad peak in the spectrum.

The other reason for confusion is the lack of systematic study by substitution of a part of constituents or comparison with the other isostructural materials. Although there were a couple of studies for the single crystals,[7–10] the group-theoretical discussion is not enough for a complete mode assignment. As described above, in order to determine which atom is associated with a certain phonon peak, it is necessary to compare the spectrum with that of the other isostructural material or partially substituted material. Here, partial substitution or change of a constituent atom by another atom corresponds to change of oscillator mass and/or force constant of the lattice vibration related with lattice constant.

In the present work we systematically investigated the optical phonon spectra of more than ten cuprate superconductors and related materials with CuO_2 plane, as well as three noncopper compounds, using the single crystals for all of the investigated materials. By comparing the spectra among various materials, most of the infrared active phonon modes are unambiguously assigned, and as a result the two main phonon modes with the highest frequencies are identified to be those of the Cu-O vibration within the plane. The quantitative analysis for the single crystal spectra enables us to estimate the effective charges which turn out to reveal a covalent character of this class of materials. In all the infrared active phonons, only the in-plane Cu-O stretching mode frequency was found to depend strongly on the Cu-O distance. It indicates that this phonon mode directly couples with the Cu $3d-$O $2p$ charge transfer electronic excitation.

II. EXPERIMENTALS

We have prepared the following single crystals: (i) (2:1:4) cuprates with $K_2(NiF)_4$ (T) structure, La_2CuO_4 and $Sr_2CuO_2X_2$ (X =Cl and Br); (ii) (2:1:4) cuprates with T' structure, L_2CuO_4 (L =Pr, Nd, Sm, Eu, and Gd) and $(Nd,Ce)_2CuO_4$; (iii) (2:1:4) cuprate with T^*-structure, $La_{1.4}Dy_{0.6}CuO_4$; (iv) other cuprates, $Ca_{0.86}Sr_{0.14}CuO_2$, $YBa_2Cu_3O_{6.1}$, $Bi_2SrLaCuO_y$; (v) noncopper 2:1:4 compounds with T structure, La_2NiO_4, $LaSrCoO_4$, and $LaSrFeO_4$. Most of the crystals were grown by the CuO-flux method except for $Sr_2CuO_2X_2$, $(Nd,Ce)_2CuO_4$ and noncopper compounds. $Sr_2CuO_2X_2$ were directly grown from the stoichiometric melt of $SrCO_3$, CuO, and SrX_2, while $(Nd,Ce)_2CuO_4$ and noncopper compounds were grown by the floating zone method. All the samples except for $Nd_{1.85}Ce_{0.15}CuO_4$ are insulating. The reducing treatment was necessary for some of the samples in order to remove the screening effect on phonons due to free carriers.

The crystal structures of these samples are illustrated schematically in Fig. 1. The (2:1:4) compounds with T structure [Fig. 1(a)] are La_2CuO_4, $Sr_2CuO_2X_2$ (X =Cl and Br), La_2NiO_4, $LaSrCoO_4$, and $LaSrFeO_4$. Among them, only La_2CuO_4 shows metallic conduction and superconductivity with $T_c \simeq 40$ K by Sr substitution for La. Other (2:1:4) compounds are Ln_2CuO_4 with T' structure shown in Fig. 1(c), which become superconductors with $T_c \simeq 25$ K when electrons are doped by substitution of Ce for the Ln atom. $(La,Dy)_2CuO_4$ is also a (2:1:4) compound but has T^* structure shown in Fig. 1(b). This structure can be regarded as a hybrid of T and T' structures in a sense that it has both of the LaO layer and oxygen fluorite layer. The latter is specific to T' structure. The isostructural T^*-$(Nd, Ce, Sr)_2CuO_4$ shows superconductivity with $T_c \simeq 25$ K. The structure of $(Ca,Sr)CuO_2$ is the simplest one among the layered perovskite cuprates, which is the alternative stacking of CuO_2 and Ca (Sr) layer [see Fig. 1(d)]. In this material, it is difficult to dope with carriers, so that superconductivity has not been realized yet.

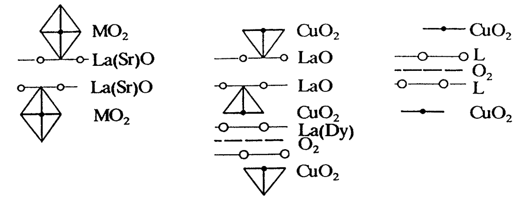

(a) T-$(La,Sr)_2MO_4$ (M=Cu,Ni,Co and Fe)

(b) T*-$(La,Dy)_2CuO_4$

(c) T'-L_2CuO_4 (L =Pr,Nd,Sm,Eu and Gd)

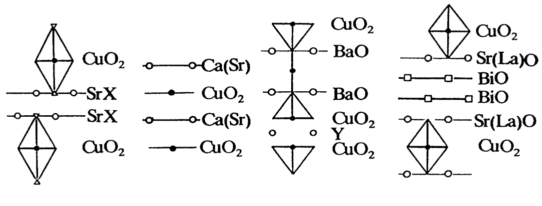

(d) $Sr_2CuO_2X_2$ (X=Cl and Br)

(e) $(Ca,Sr)CuO_2$

(f) $YBa_2Cu_3O_6$

(g) $Bi_2SrLaCuOy$

FIG. 1. Schematical crystal structures of the investigated materials (cross section along the c axis). The solid circle denotes the Cu atom and the open circle denotes the lanthanide or alkaline earth atom.

$YBa_2Cu_3O_y$ is so-called 1:2:3 compound which shows superconductivity with $T_c = 90$ K when the oxygen content is 7. $Bi_2SrLaCuO_y$ has the double BiO layer between the CuO_6 octahedra, resulting in the long c axis [Fig. 1(f)]. When La is completely substituted by Sr, superconductivity appears with $T_c = 20$ K.

The sample surfaces were carefully mirror polished with use of the Al_2O_3 powder with acetone. The sample areas of ab direction are large enough for infrared measurement, typically 3×5 mm^2, while the thickness is so small that the spectrum for $E \| c$ cannot be measured for most of the samples except for Nd_2CuO_4, $(Nd,Ce)_2CuO_4$, Pr_2CuO_4, and La_2NiO_4 with the c-direction dimension of 1–5 mm. The reflectivity spectra were measured at room temperature in the wave number range 50–4000 cm^{-1} by using Bruker 113V spectrometer and Bomem DA3 Microscope FTIR system. As a reference, the Au evaporated thick film was used.

III. RESULTS AND ANALYSIS

A. Phonon spectra for the (2:1:4) cuprates with $T(K_2NiF_4)$ structure

The reflectivity phonon spectrum of La_2CuO_4 for $E \perp c$ is shown in Fig. 2. The solid circles represent the experimental data and the solid curves were calculated by fitting procedure based on the oscillator model where the

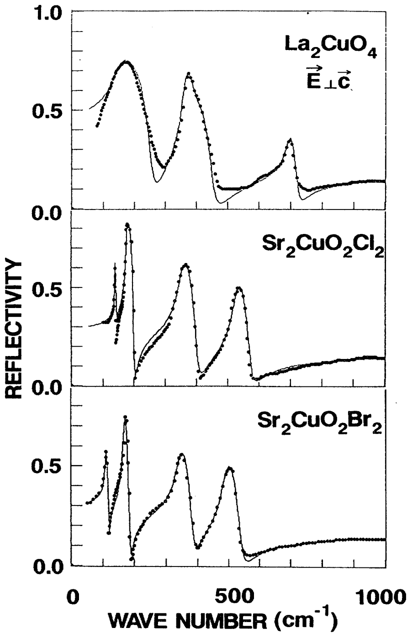

FIG. 2. Phonon spectra of (2:1:4) cuprates with $K_2NiF_4(T)$ structure for **E**⊥c.

dielectric function $\epsilon(\omega)$ is represented as

$$\epsilon(\omega)=\epsilon_\infty+\sum_j \frac{S(j)\omega_{\mathrm{TO}}^2(j)}{\omega_{\mathrm{TO}}^2(j)-\omega^2-i\omega\gamma(j)} . \quad (1)$$

The obtained fitting parameters are listed in Table I. The shoulder structure at around 400 cm^{-1} in the spectrum is so weak that the determined phonon frequency and oscillator strength corresponding to this peak may include some error. These results are almost the same as that previously reported by Collins *et al.*,[7] although they did not recognize the little shoulder mentioned above.

The actual symmetry of La_2CuO_4 is orthorhombic at room temperature due to rigid rotational distortion of the CuO_6 octahedra, but the effect of this kind of distortion should be small on the phonon and/or electronic structure, as supported by the result that the number of the observed phonon peaks is appreciably smaller than that expected for orthorhombic symmetry. From the group theory, seven infrared active phonon modes are expected to be observed in tetragonal D_{4h}^{17} symmetry, as represented as $\Gamma_{\mathrm{opt}}=3A_{2u}+4E_u+2A_{1g}+2E_g+B_{2u}$. The supposed eigenvector corresponding to each mode was calculated by Pintschovius *et al.*,[11] as illustrated in Fig. 3. These phonon modes can be classified in three types, following the cubic perovskite case; (i) external mode which is a translational vibration of *A*-site atom layer against the CuO_2 unit as illustrated in Figs. 3(d) and 3(g), (ii) Cu-O stretching mode which is in Cu-O *bond distance* modulation as in Figs. 3(a) and 3(e), and (iii) Cu-O bending mode which is the Cu-O *bond angle* modulation as in Figs. 3(b), 3(c), and 3(f). In all the spectra of La_2CuO_4 reported so far, one of the seven modes has not been observed clearly. As indicated by the results for single crystals in this work and Ref. 7, the missed one phonon is one of the four E_u modes with **E**⊥c. Several interpretations are possible for this phonon missing. One of them is that one phonon peak is overlapped with the other phonon peak, for example, with the broad peak centered at 180 cm^{-1} or with the peak at 360 cm^{-1}. Another interpretation is that the mode in question must be located in the low-frequency region out of the measuring range.[10] The latter may be possible when the observed reflectivity rises toward lower frequency. However, in the case of La_2CuO_4, the oxygen content tends to deviate from the stoichiometric value under the normal synthesis condition, resulting in the small density of carriers. Therefore, the possibility of the free carrier effect cannot be ruled

TABLE I. Fitting parameters for the spectra of (2:1:4) cuprates with *T* and *T** structures for **E**⊥c in Figs. 2 and 7.

	La_2CuO_4	$Sr_2CuO_2Cl_2$	$Sr_2CuO_2Br_2$	$(La,Dy)_2CuO_4$
$\omega_{\mathrm{TO}}(1)$ (cm^{-1})	145	176	167	138
$S(1)/\epsilon_\infty$	3.87	0.49	0.36	1.54
$\gamma(1)$ (cm^{-1})	45	5	6	48
$\omega_{\mathrm{TO}}(2)$ (cm^{-1})	(400)	140	111	
$S(2)/\epsilon_\infty$	(0.05)	0.06	0.29	
$\gamma(2)$ (cm^{-1})	(60)	1	5	
$\omega_{\mathrm{TO}}(3)$ (cm^{-1})	360	351	342	359
$S(3)/\epsilon_\infty$	0.30	0.39	0.35	0.75
$\gamma(3)$ (cm^{-1})	20	26	27	52
$\omega_{\mathrm{TO}}(4)$ (cm^{-1})	695	525	488	598
$S(4)/\epsilon_\infty$	0.06	0.14	0.17	0.12
$\gamma(4)$ (cm^{-1})	27	27	31	92
ϵ_∞	6.0	5.5	5.5	6.0

out for the reflectivity rise in the lower frequency range.

Concerning this problem, the spectra of $Sr_2CuO_2X_2$ (X = Cl and Br) with T structure provide useful information. As shown in Fig. 2, four distinct phonon peaks can be observed in these spectra. The substitution of Cl or Br for the apical oxygen corresponds to increasing of the phonon activity of the bending mode associated with the apical atoms [see Fig. 3(c)]. Therefore, it is concluded that the phonon which we cannot see clearly in the spectrum of La_2CuO_4 is the apex bending mode as illustrated in Fig. 3(c). The oscillator strength of this mode may be small because it originates from the inactive F_{2u} mode in the cubic symmetry. The small activity of the phonon associated with the apical oxygen was also speculated by Crawford *et al.*[8] Considering that this phonon is observed at 230 cm^{-1} in La_2NiO_4 as described later, it is possible that the apex bending phonon overlaps the dominant phonon at 140 cm^{-1}.

It should be noticed in Table I that the second highest phonon frequency is almost the same value (360 cm^{-1}) among them. Therefore, this phonon mode with the common frequency is no doubt a vibrational mode associated with the common structure, namely, CuO_2 plane. This fact is shown more clearly below by comparing the results for various other cuprates.

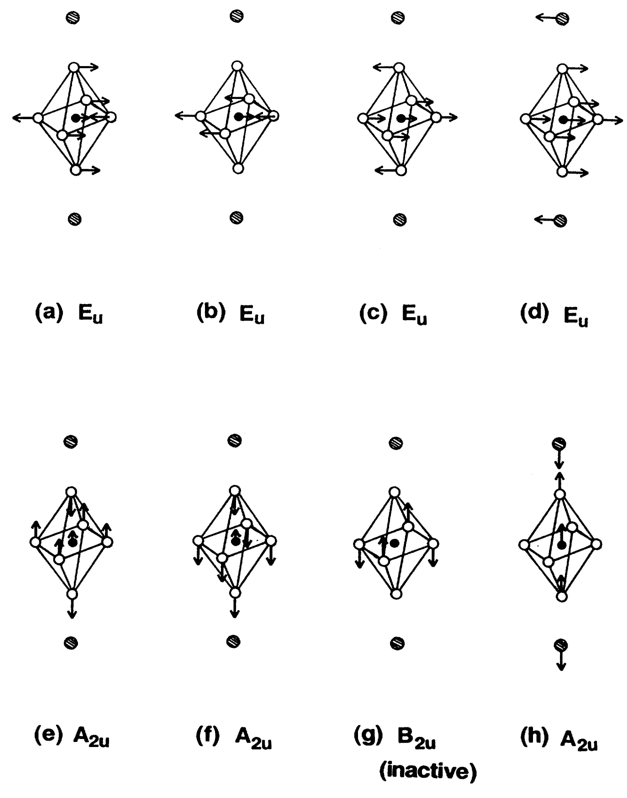
(a) Eu (b) Eu (c) Eu (d) Eu

(e) A2u (f) A2u (g) B2u (inactive) (h) A2u

FIG. 3. Atomic displacements of the infrared active phonon modes for K_2NiF_4 structure with D_{4h}^{17} symmetry, which were calculated by Pinyschovius *et al.* (Ref. 11). (a)–(d) correspond to the vibrational modes perpendicular to the c axis (E_u) and (e)–(g) correspond to those parallel to the c axis (A_{2u}). (h) show the inactive mode (B_{2u}).

B. Phonon spectra for (2:1:4) cuprates with T' structure

Figure 4 summarizes the phonon spectra of L_2CuO_4 (L = Nd, Pr, Sm, Eu, and Gd) for E⊥c. These have the common spectral profile consisting of the small peak at 130 cm^{-1}, the wide band with the sharp cut at around 350 cm^{-1} and the large peak at around 500 cm^{-1}, which reflects the common T' structure. This structure has no apex oxygen but fluorite-type oxygen layer on both sides of the CuO_2 plane. Since the space group is D_{4h}^{17}, the same as that for T structure, there are four infrared active modes ($4E_u$) for E⊥c all of which are clearly observed in the spectra.

The fitting parameters are listed in Table II. It can be seen that the value of $\omega_{TO}(1)$, as well as of $\omega_{TO}(2)$, are almost the same among the five compounds, while the value of $\omega_{TO}(4)$ depends on the lattice constant a. The difference in the masses of lanthanide atoms being small among the five compounds, it is easily understood that the TO-phonon frequency of the external mode, probably corresponding to $\omega_{TO}(1)$, depends little on the compounds. The other three modes are supposed to be associated with the common structure composed of Cu and O.

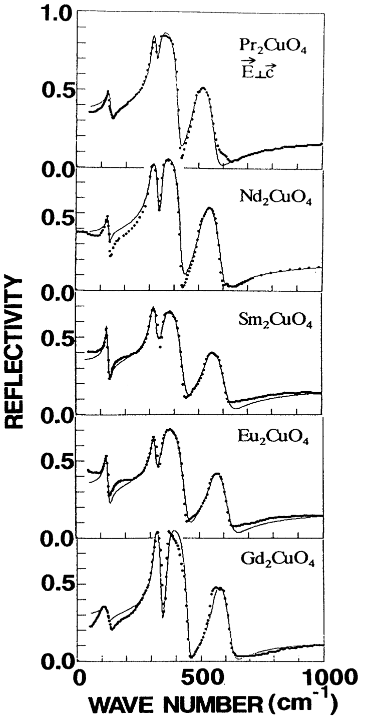

FIG. 4. Phonon spectra of L_2CuO_4 with T' structure for E⊥c (L=Pr, Nd, Fu, Sm, and Gd).

TABLE II. Fitting parameters for the spectra of Ln_2CuO_4 with T' structure for **E**⊥**c** in Fig. 4. (The smaller value of ϵ_∞ for Gd_2CuO_4 is derived from the low reflectivity in the higher-frequency region. This may not be intrinsic but due to the roughness of the sample surface.)

	Pr_2CuO_4	Nd_2CuO_4	Sm_2CuO_4	Eu_2CuO_4	Gd_2CuO_4
$\omega_{TO}(1)$ (cm^{-1})	128	130	125	123	118
$S(1)/\epsilon_\infty$	0.37	0.16	0.35	0.39	0.21
$\gamma(1)$ (cm^{-1})	15	8	8	11	20
$\omega_{TO}(2)$ (cm^{-1})	305	304	311	312	315
$S(2)/\epsilon_\infty$	0.90	1.00	0.52	0.32	0.69
$\gamma(2)$ (cm^{-1})	9	17	16	12	8
$\omega_{TO}(3)$ (cm^{-1})	332	350	359	356	370
$S(3)/\epsilon_\infty$	0.34	0.29	0.50	0.65	0.35
$\gamma(3)$ (cm^{-1})	19	15	42	37	13
$\omega_{TO}(4)$ (cm^{-1})	486	512	540	555	555
$S(4)/\epsilon_\infty$	0.18	0.18	0.17	0.16	0.15
$\gamma(4)$ (cm^{-1})	50	48	64	56	38
ϵ_∞	6.5	6.5	6.0	6.0	5.0

The spectrum of T' material for **E**||**c** was measured for Nd_2CuO_4 and Pr_2CuO_4, as shown in Fig. 5. The fitting parameters are listed in Table III. Here, three phonon peaks are observed, corresponding to the three A_{2u} modes in the group theory.

The spectrum of Ce-doped $Nd_{0.85}Ce_{0.15}CuO_4$ was also measured for both directions **E**⊥**c** and **E**||**c**. As seen in Fig. 6, the strong anisotropy was observed, which was also reported for the single crystal $(La,Sr)_2CuO_4$.[7] For $E \perp c$ the plasmon due to the doped carrier dominates the spectrum and no phonon peak is observed, while the spectrum for $E \| c$ is almost the same as that of undoped Nd_2CuO_4 except for a slight shift of its frequency.

C. Phonon spectrum of $(La,Dy)_2CuO_4$ with T^* structure

A good insulating single crystal of T^* material was successfully obtained for $(La,Dy)_2CuO_4$. For other T^* materials we could not completely remove the free carriers at room temperature. The spectrum of $(La,Dy)_2CuO_4$ for **E**⊥**c** is shown in Fig. 7 and the fitting parameters are in Table I. Disorder introduced by substitution of a part of La for Dy broadens the phonon peaks. Since the space group of this material is D_{4h}^7, there should be six infrared active modes in the spectrum for **E**⊥**c**, whereas only three broad peaks can be observed in Fig. 7. As described in Sec. III A, the phonon mode associated with the apical oxygen may probably be weak in strength and/or overlap the other phonon.

D. Phonon spectra of other cuprates

The spectrum of $Ca_{0.86}Sr_{0.14}CuO_2$ with simpler layered structure is also interesting. The space group of this material is D_{4h}^1 and there are five infrared-active modes, namely, $\Gamma_{opt} = 2A_{2u} + 3E_u$. As shown in Fig. 8(a), all the

TABLE III. Fitting parameters for the spectra of T and T' compounds for **E**||**c** in Figs. 5, 6(b), and 10.

	La_2NiO_4	Pr_2CuO_4	Nd_2CuO_4	$(Nd,Ce)_2CuO_4$
$\omega_{TO}(1)$ (cm^{-1})	280	130	130	130
$S(1)/\epsilon_\infty$	2.72	0.33	0.81	0.51
$\gamma(1)$ (cm^{-1})	25	15	25	5
$\omega_{TO}(2)$ (cm^{-1})	370	290	275	270
$S(2)/\epsilon_\infty$	0.03	1.74	1.86	2.29
$\gamma(2)$ (cm^{-1})	10	37	27	32
$\omega_{TO}(3)$ (cm^{-1})	515	500	513	500
$S(3)/\epsilon_\infty$	0.06	0.08	0.10	0.06
$\gamma(3)$ (cm^{-1})	25	35	24	27
ϵ_∞	5.0	4.0	4.5	4.0

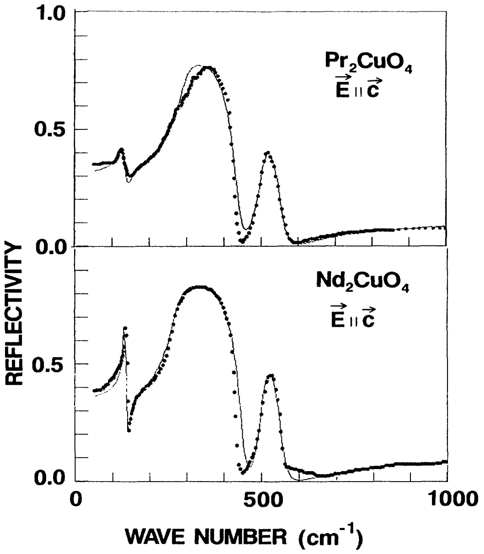

FIG. 5. Phonon spectra L_2CuO_4 with T' structure for E||c (L=Pr and Nd).

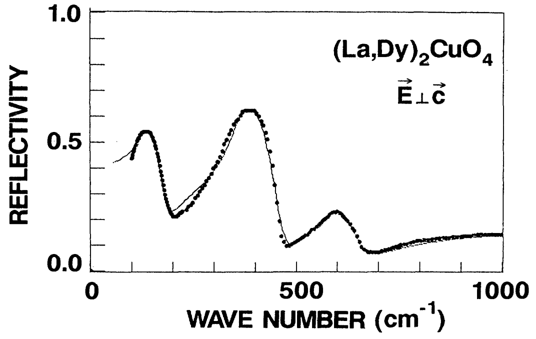

FIG. 7. Phonon spectrum of $La_{1.4}Dy_{0.6}CuO_4$ with T^* structure for E⊥c.

three phonon modes ($3E_u$) are observed clearly in the spectrum for E⊥c. The fitting parameters are listed in Table IV. These three modes can also be classified into the above described external, bending , and stretching-type modes. Among the observed three phonons, the lowest phonon frequency (230 cm^{-1}) is considerably higher than that for La_2CuO_4 (140 cm^{-1}). Certainly, this peak corresponds to the external mode associated with the vibration of Ca atom, because the reduced mass of this mode is much smaller than the corresponding one with La atom. The other two peaks at higher frequencies are supposed to correspond to the Cu-O stretching and the Cu-O bending mode.

One of the typical high-T_c cuprates other than the (2:1:4) compounds is the so-called (1:2:3) compound such as $YBa_2Cu_3O_y$. The phonon spectrum of insulating $YBa_2Cu_3O_{6.1}$ for E⊥c is shown in Fig. 8(b) and the fitting parameters are in Table IV. Although there should be six infrared active modes ($6E_u$) for E⊥c, that is, $\Gamma_{\text{opt}}=5A_{2u}+6E_u+4A_{1g}+B_{1g}+5E_g+B_{2u}$, only five phonon peaks can be observed in Fig. 8, which is in good agreement with the previous Crawford result.[8] As in the (2:1:4) compounds with T and T^* structures, the bending

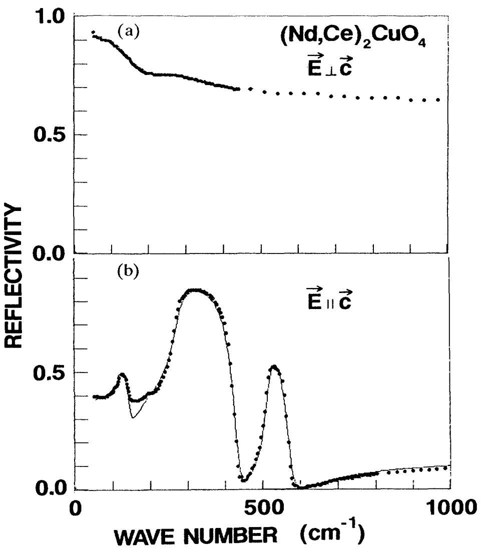

FIG. 6. Phonon spectra of Ce-doped $Nd_{1.85}Ce_{0.15}CuO_4$ both for E⊥c (a) and E||c (b). The spectrum for E⊥c (a) dominated by the free carrier plasma shows the metallic property of the sample, which is in contrast to the insulating spectrum for E||c.

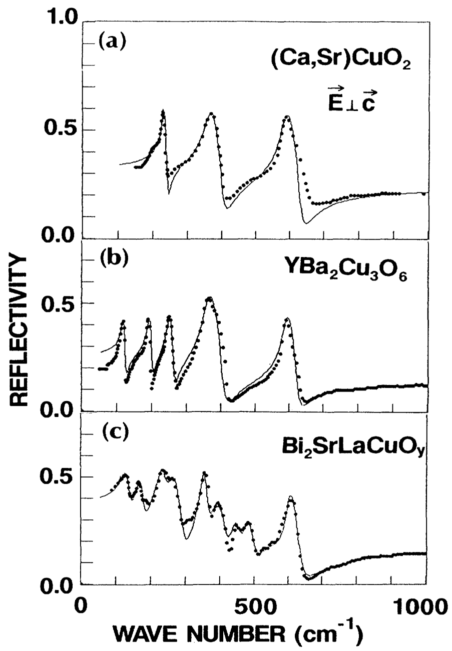

FIG. 8. Phonon spectra of $(Ca,Sr)CuO_2$ (a), $YBa_2Cu_3O_y$ (b), and $Bi_2SrLaCuO_y$ (c) for E⊥c.

TABLE IV. Fitting parameters for the spectra of (Ca,Sr)CuO$_2$, YBa$_2$Cu$_3$O$_{6.1}$, and Bi$_2$SrLaCuO$_y$ for **E**⊥c in Fig. 8. The listed two values for each mode of Bi$_2$SrLaCuO$_y$ correspond to those of the double peaks.

	(Ca,Sr)CuO$_2$	YBa$_2$Cu$_3$O$_{6.1}$	Bi$_2$SrLaCuO$_y$
$\omega_{\mathrm{TO}}(1)$ (cm^{-1})	230	118	130,170
$S(1)/\epsilon_\infty$	0.18	0.21	0.61,0.32
$\gamma(1)$ (cm^{-1})	10	9	22,20
$\omega_{\mathrm{TO}}(2)$ (cm^{-1})		193	230,260
$S(2)/\epsilon_\infty$,		0.15	0.38,0.33
$\gamma(2)$ (cm^{-1})		10	25,40
$\omega_{\mathrm{TO}}(3)$ (cm^{-1})	360	357	350,390
$S(3)/\epsilon_\infty$	0.31	0.31	0.15,0,13
$\gamma(3)$ (cm^{-1})	31	30	17,40
$\omega_{\mathrm{TO}}(4)$ (cm^{-1})	583	588	560,600
$S(4)/\epsilon_\infty$	0.15	0.10	0.07,0.05
$\gamma(4)$ (cm^{-1})	30	26	110,23
$\omega_{\mathrm{TO}}(5)$ (cm^{-1})		250	445,480
$S(5)/\epsilon_\infty$		0.17	0.05,0.04
$\gamma(5)$ (cm^{-1})		14	30,30
ϵ_∞	8.5	5.0	6.0

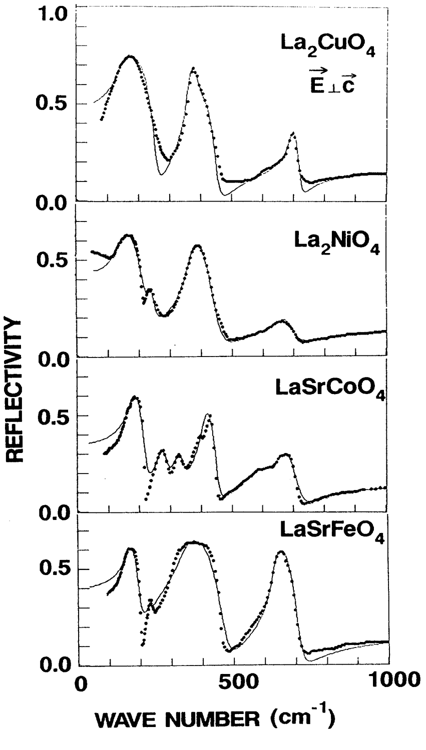

FIG. 9. Phonon spectrum of (La,Sr)$_2M$O$_4$ for **E**⊥c. (M =Cu, Ni, Co, and Fe).

mode associated with the apical oxygen may possibly be weak. It is noticeable that also for the materials in Table IV the second highest frequency phonon is located at around 360 cm^{-1}, as in the T and T^* structures. It seems to be the common frequency among the layered cuprates.

Another type of typical high-T_c cuprates consists of Bi based compounds. In Fig. 8(c) is shown the spectrum of Bi$_2$SrLaCuO$_{6.5}$ for **E**⊥c. Although the spectrum is full of structure, it can be regarded to be composed of the five or six phonon peaks, each having a doublet. In an undistorted structure, there should be six infrared active phonon modes for **E**⊥c. The peak splitting may have arisen from the distortion in the double BiO layers.

E. Phonon spectra of noncopper compounds with T structure

For discussion about the phonon spectra of cuprates, it is of great help to compare them with the spectra of noncopper compounds. In Fig. 9 are summarized the spectra of (2:1:4) compounds with T structure, La$_2$CuO$_4$, La$_2$NiO$_4$, LaSrCoO$_4$, and LaSrFeO$_4$ for **E**⊥c and their fitting parameters are in Table I and V. Comparing our

TABLE V. Fitting parameters for the spectra of (La,Sr)MO$_4$ (M =Ni, Co, and Fe) in Fig. 9. For La$_2$NiO$_4$, the free carrier plasma term was added to the dielectric function in Eq. (1) in fitting, that is,

$$\epsilon(\omega)=\epsilon_\infty-\frac{\omega_p^2}{\omega^2+i\omega\gamma_p}+\sum_j\frac{S(j)\omega_{\mathrm{TO}}^2(j)}{\omega_{\mathrm{TO}}^2(j)-\omega^2-i\omega\gamma(j)} .$$

	La$_2$NiO$_4$	LaSrCoO$_4$	LaSrFeO$_4$
$\omega_{\mathrm{TO}}(1)$ (cm^{-1})	150	178	165
$S(1)/\epsilon_\infty$	2.24	1.20	1.30
$\gamma(1)$ (cm^{-1})	48	34	30
$\omega_{\mathrm{TO}}(2)$ (cm^{-1})	236	276	230
$S(2)/\epsilon_\infty$	0.04	0.13	0.04
$\gamma(2)$ (cm^{-1})	27	34	15
$\omega_{\mathrm{TO}}(3)$ (cm^{-1})	367	331	340
$S(3)/\epsilon_\infty$	0.39	0.11	1.08
$\gamma(3)$ (cm^{-1})	39	37	65
$\omega_{\mathrm{TO}}(3')$ (cm^{-1})		410	
$S(3')/\epsilon_\infty$		0.22	
$\gamma(3')$ (cm^{-1})		30	
$\omega_{\mathrm{TO}}(4)$ (cm^{-1})	675	668	630
$S(4)/\epsilon_\infty$	0.05	0.10	0.17
$\gamma(4)$ (cm^{-1})	65	62	33
$\omega_{\mathrm{TO}}(4')$ (cm^{-1})		609	
$S(4')/\epsilon_\infty$		0.07	
$\gamma(4')$ (cm^{-1})		100	
ω_p (cm^{-1})	700		
γ_p (cm^{-1})	1000		
ϵ_∞	5.4	5.5	5.5

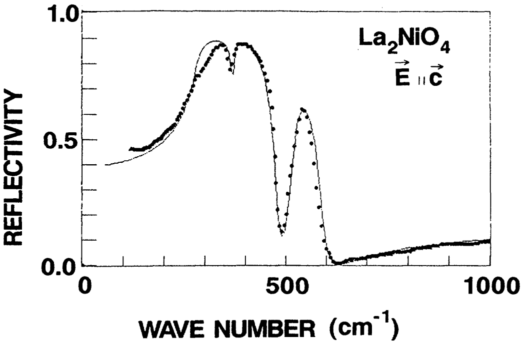

FIG. 10. Phonon spectrum of La$_2$NiO$_4$ for E||c.

result for La$_2$NiO$_4$ with the previously reported one by Bassat *et al.*,[12] all the phonon peaks for E⊥c can be more clearly observed in our data because we were successful in suppressing considerably the free carrier plasma by reducing oxygen content in the nonstoichiometric La$_2$NiO$_{4+y}$. In contrast to the spectrum of La$_2$CuO$_4$, the distinct feature is that there are four phonon peaks for E⊥c, probably including the apex bending mode. Besides the phonon structures, two electronic contributions are observed in this spectrum. The first one is the free carrier plasma due to the small excess oxygen which raises the reflectivity in the lower energy region. The second one is the broad peak in the midinfrared region, out of the range in Fig. 9. The latter midinfrared absorption is also commonly observed in the lightly doped layered cuprates[13] and is supposed to be intrinsic to the system strongly influenced by the many-body effect such as electron correlation or electron-phonon interaction. For La$_2$NiO$_4$ we could also measure the spectrum for E||c shown in Fig. 10. The fitting parameters are in Table III, together with the other E||c spectrum.

In LaSrCoO$_4$, there supposedly exists the high-spin and low-spin ordering. Due to its structural distortion coupled with this ordering, so-called breathing mode distortion, the phonon peaks are split-off. The spectrum of LaSrFeO$_4$ has a particular wide phonon band, which seems to be distinctively different from the other three. This may suggest the different bonding state or the different electronic configuration of this material from other materials.

IV. DISCUSSIONS

A. Phonon modes

In our preliminary work on the layered cuprates with single CuO$_2$ plane,[14] all the phonon modes for E⊥c were unambiguously assigned. Increasing the sample variety, the present work has confirmed this assignment. Regarding that the various structures of layered cuprates are derived basically from oxygen deficient perovskites, their phonon modes should have essentially the same character as those of the cubic perovskite which has three infrared active modes (stretching, bending, and external modes) and no Raman-active mode.

As described above, in spite of the structural variety, the phonon modes of the layered cuprates can be classified into the following common types corresponding to the three in the cubic perovskite case. Firstly, we assign the phonon modes for E⊥c. (i) Two CuO$_2$ in-plane modes (stretching and bending modes): Since both of them are mainly the oxygen vibrations, their frequencies are expected to be high. In Fig. 11, the TO-phonon frequencies of Mode 4 with the highest frequency and Mode 3 with second highest frequency are plotted against the lattice constant *a* for all the investigated materials. As shown in this figure, the frequency of Mode 4 is strongly dependent on the Cu-O distance within the plane, whereas the frequency of Mode 3 is almost constant among these materials. Similar lattice constant dependence of the highest frequency was also reported by Sreedhar *et al.*[15] In the simple model where neutral atoms are vibrating in a periodic harmonic potential, the phonon frequency depends on the lattice constant as $\omega_{\mathrm{TO}}^2 \propto a^{-3}$. The dotted lines in Fig. 11 represent the reference curves $\omega_{\mathrm{TO}} = K(a/4.0)^{-3/2}$ where $K_1 = 645$ cm^{-1}, $K_2 = 480$ cm^{-1}, and $K_3 = 340$ cm^{-1}. Comparing

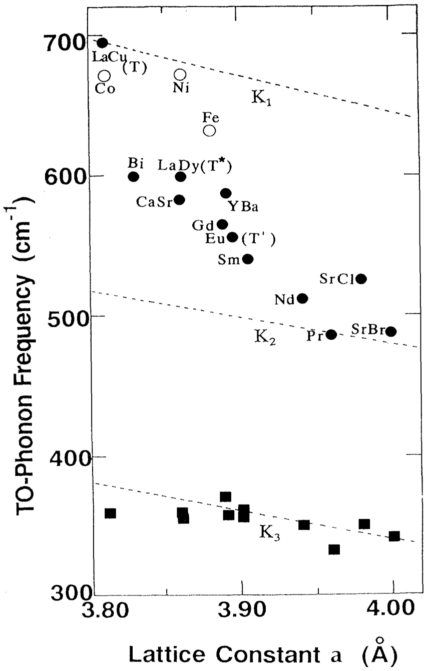

FIG. 11. The highest two TO-phonon frequencies $\omega_{\mathrm{TO}}(3)$ (solid square) and $\omega_{\mathrm{TO}}(4)$ (solid circle) plotted against the lattice constant *a* for all the investigated cuprates. The data denoted by open circles are for $\omega_{\mathrm{TO}}(4)$ of the investigated noncopper oxides. The dashed lines represent the relation $\omega_{\mathrm{TO}} = K(a/4.0)^{-3/2}$ with $K_1 = 645$ cm^{-1}, $K_2 = 480$ cm^{-1}, and $K_3 = 340$ cm^{-1}. The plotted *a* value for orthorhombic La$_2$CuO$_4$ is the average of the lattice parameters *a* and *b*.

the experimental results with these lines, $\omega_{\mathrm{TO}}(4)$ is found to vary much more sensitively against a. From this fact, we have assigned the highest frequency phonon (Mode 4) to the stretching type mode and the second highest one (Mode 3) to the bending type mode, because the frequency of the stretching mode which is the Cu-O bond distance modulation, may possibly be affected by the interaction with electronic system which might also be modulated by the change of Cu-O bond distance.

(ii) External mode and out-of-plane oxygen mode: As shown in Fig. 3, the reduced mass of the external mode should be the heaviest among all the optical phonon modes because it is the vibration of the heavier lanthanide or alkaline earth atom against the CuO unit. Therefore, the phonon with the lowest frequency is assigned to this mode, except for $\mathrm{Sr_2CuO_2}X_2$ ($X=\mathrm{Cl}$ and Br) where the reduced mass of the external mode is comparable to that of the apex Cl(Br)-bending mode. In Fig. 12 are plotted the square of external mode frequency with $\mathbf{E}\perp\mathbf{c}$ against the inverse of the A-site atomic weight for all of the investigated cuprates. Strictly speaking, the atomic displacement pattern is slightly different among the compounds, depending on the crystal structure and/or the masses of the constituent atoms. However, the results in Fig. 12 show a systematic dependence of the TO-phonon frequency on the mass of A-site atom. It is a strong experimental evidence that this phonon mode corresponds to the vibration of A-site atom, that is, the external type mode. The other intermediate frequency phonons can be assigned to the vibration of the out-of-layer oxygen. In the case of T' compounds, the specific wide phonon band around 300 cm^{-1} (Mode 2), is supposed to correspond to the vibrational mode of the oxygen in the fluorite layer. In the case of the compounds with the CuO octahedron or pyramid, the bending mode associated with the apex atoms is expected to be observed from the group theory. In $\mathrm{Sr_2CuO_2}X_2$ ($X=\mathrm{Cl}$ and Br), the lowest frequency phonon is assigned to this apex bending mode, because its frequency is most sensitive to the mass of the apex atom (Cl or Br) as seen in Table I. In the spectra of $\mathrm{La_2CuO_4}$, $\mathrm{(La,Dy)_2CuO_4}$, and $\mathrm{YBa_2Cu_3O_{6.1}}$, the apex oxygen bending mode cannot be clearly observed. Since this mode is optically silent in the original cubic perovskite, its oscillator strength may be small.

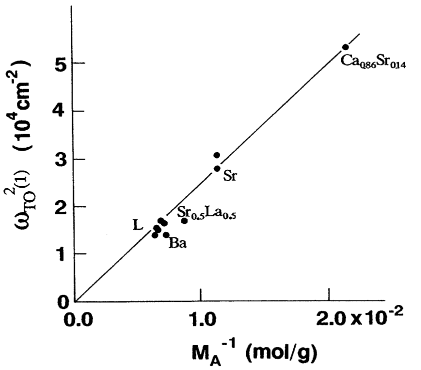

FIG. 12. The TO-phonon frequencies of the external mode $\omega_{\mathrm{TO}}(1)$ plotted against the inverse of the A-site atomic weight M_A for all the investigated cuprates ($L=\mathrm{Pr}$, Nd, Sm, Eu, and Gd).

The phonon spectra of $\mathrm{LaSrCoO_4}$ and $\mathrm{LaSrFeO_4}$ for $\mathbf{E}\perp\mathbf{c}$ are also roughly composed of three phonon bands, corresponding to the above three modes (stretching, bending, and external), although in $\mathrm{LaSrCoO_4}$ the phonon peaks are split due to the lattice distortion. The spectrum of $\mathrm{La_2NiO_4}$ is very similar to that of $\mathrm{La_2CuO_4}$ except for the appearance of the apex bending mode at 220 cm^{-1}. The reason why the infrared activity of this mode is so different between them remains an open question.

(iii) c-axis modes: The spectra for $\mathbf{E}\parallel\mathbf{c}$ were obtained only for the (2:1:4) compound with T and T' structures. The eigenvectors of three infrared active modes for this direction are illustrated in Fig. 3. These can be also called as external, stretching, and bending type modes. Similar to the phonons for $\mathbf{E}\perp\mathbf{c}$, the highest frequency phonon is assigned to the Cu-O stretching mode. In the case of T' structure, this mode corresponds to the relative motion of fluorite-type oxygen layer and Cu layer. Based on the reduced mass argument, the lowest and the middle frequency phonons are assigned to the external mode and the bending mode, respectively. However, concerning the T-structure spectrum, it is not clear why the vibration of the A-site atom is not seen clearly or has high frequency.

B. Effective charges

1. *Bonding ionicity and extended effective charge*

The effective charge is an important quantity in discussion of the bonding ionicity. However, the evaluation of the effective charge is very difficult for the material composed of more than two kinds of atoms. The transverse effective charge e_T^*, which is directly related to the phonon band width or oscillator strength, is defined only for "binary" compound. For a ternary compound, Scott introduced the extended effective charge Z_k defined as follows:[16]

$$\sum_i [\omega_{\mathrm{LO}}^2(j)-\omega_{\mathrm{TO}}^2(j)]=\frac{4\pi}{V}\sum_k (Z_k e)^2/Mk \ , \tag{2}$$

$$\sum_k Z_k=0 \ , \tag{3}$$

where j denotes the phonon mode, V is a unit cell volume, and the k sum is over all atoms with the mass M_k and the effective charge $Z_k e$. In the binary compound, this effective charge Ze is related to the transverse effective charge e_T^* as $\mathrm{Ze}=\epsilon_\infty^{-1/2}e_T^*$. Compensating the dynamical contribution in e_T^* by the optical dielectric constant factor, Ze predominantly represents the *static* contribution to the lattice dynamics, which can be seen, for example, by the fact that Ze scales well to Phillips' ionicity in the various diatomic compounds.[17]

Except for the special case where a certain atom is associated with only one vibrational mode,[17] the above equation cannot be solved precisely because there are only two equations with many unknown parameters Z_k's. In the oxices where the masses of other constituents are much heavier than the oxygen mass, such as La_2MO_4 with T, T', and T^* structure, and $YBa_2Cu_3O_{6.1}$, it may be permitted to neglect the terms other than the oxygen term on the right-hand side of Eq. (2). The error due to this neglect is about 10%. In the compounds with other lighter atoms such as (Ca,Sr)CuO_2 and $Sr_2CuO_2X_2$ (X = Cl and Br), this neglect leads to a considerable overestimation of Z_0 value. Furthermore, it should be noted that the obtained Z_0 value is the average for all the oxygen sites.

Adopting this approximation, the oxygen effective charge Z_0's were estimated for various (2:1:4)-compounds with T, T', and T^* structure and $YBa_2Cu_3O_{6.1}$ by using the parameters in Tables I, III, IV, and V, where LO-phonon frequency $\omega_{LO}^2(j)$ was defined as $\omega_{LO}^2(j)=[1+S(j)/\epsilon_\infty]\omega_{TO}^2(j)$. As shown in Table VI, the Z_0 values are considerably small, about half of the full valence 2.0 for the cuprates. These are comparable to $|Z_0|=1.1$ in the typical covalent perovskite oxide $BaBiO_3$,[18] but remarkably smaller than $|Z_0|=1.8$ in the ionic perovskite oxide $KTaO_3$.[17] These small values of $|Z_0|$ in the cuprates indicate the highly covalent character of these materials. If this covalency is attributed to the fact that the energy level of Cu is close to that of oxygen, it must be affected by changing the B-site atom (Cu) to Ni, Co, and Fe. Although the energy level difference between the oxygen and these metal atoms must systematically change, the ionicity estimated by Z_0 does not change appreciably. Among them, the value of $|Z_0|$ for $LaSrFeO_4$ is larger than that for cuprates, which indicates a relative ionic character of $LaSrFeO_4$. The discontinuous change in Z_0 between Co and Fe, which was also seen in the phonon spectra of cubic perovskite $LaMO_3$ (M = Co and Fe),[19] may suggest the discontinuous change in the electronic states. It was also suggested by the vacuum ultraviolet region spectra of these materials.[20] In contrast to Fe^{3+} with $3d^5$ configuration where the high-spin state is stable, Co^{3+} with $3d^6$ may be a delicate state where the high-spin state is in competition with the low-spin state. This drastic change in the electronic configuration may possibly result in the discontinuous change of the optical spectra from far-infrared to vacuum-ultraviolet region.

TABLE VI. Oxygen effective charges Z_0 for various cuprates and the noncopper (2:1:4) compounds which were estimated from the parameters in Tables I, II, IV, and V as described in the text.

	La_2CuO_4	$(La,Dy)_2CuO_4$	Pr_2CuO_4	$YBa_2Cu_3O_y$
Z_0	−1.1	−1.2	−1.2	−1.0

	La_2NiO_4	$LaSrCoO_4$	$LaSrFeO_4$
Z_0	−1.0	−1.1	−1.3

2. Transverse effective charge and dynamical contribution to the phonon system

The transverse effective charge e_T^*, another important effective charge, is defined for a binary compound as

$$e_T^{*2}=\frac{M}{4\pi N}S\omega_{TO}^2 . \tag{4}$$

In general, e_T^* includes both static and dynamical contributions, the former being the contribution from the rigid ion core and the latter due to redistribution of valence electrons. Approximating the stretching mode vibration as two-body problem of Cu and O, e_T^* for this mode was calculated for each material.

In Fig. 13 the estimated e_T^*'s for all the investigated cuprates are plotted against the lattice constant. Firstly, it is found that the estimated e_T^* values exceed the nominal Cu valence of 2.0e. This indicates a considerable amount of dynamical contribution to this effective charge. Secondly, these values are distributed from 2.05e for La_2CuO_4 to 3.00e for $Sr_2CuO_2Br_2$. This difference in e_T^* among the materials is too large to be ignored, in contrast to the small difference in Z_0 among them. Thirdly, although the data show little scatter due to the ambiguity of the oscillator strength, a clear correlation between e_T^* and a can be observed in Fig. 13. It suggests that the dynamical contribution from the electronic system is predominantly affected by the lattice constant a. This strong a dependence of e_T^* is similar to that of the stretching mode frequency, which may suggest that the latter is also affected by the change of electronic environment induced by the change of a.

A model for transverse effective charge was reported for binary semiconductors by Katayama and Kawamura.[21] According to them, using the Penn model, e_T^* is represented as

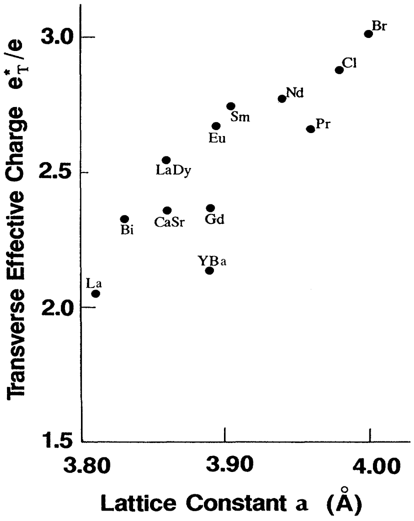

FIG. 13. The transverse effective charge plotted against the lattice constant a for all the investigated materials, which is defined for the stretching-mode phonon as described in the text.

$$e_T^* \sim e \left[\frac{Z_1 - Z_2}{2} + \frac{\Xi}{E_G} \right] , \tag{5}$$

where Z_1 and Z_2 are the valence of two ions, Ξ is the deformation potential corresponding to the relevant phonon mode, and E_G is the average energy gap. The first term represents the static contribution while the second represents the dynamical one. In the layered cuprates, the first term is supposed to be not large and not sensitive to a, because, as described in the previous subsection, the oxygen effective charge $|Z_0|e$ is relatively small ($\sim 1.0e$) and is almost the same among the investigated cuprates. Therefore, the drastic increase of e_T^* with increasing a is attributed to the drastic change of the second term, a contribution from the coupling with the electronic system.

C. Optical phonons and electronic structure in the CuO_2 plane

As shown in Fig. 11 the most outstanding feature of the phonons within the CuO_2 plane is the strong a dependence of the stretching mode frequency. If the a dependence of the phonon frequency is approximated as $\omega \sim a^{-\alpha}$, the power α is roughly estimated to be 7. Similar strong a dependence of the stretching mode frequency is observed by the hydrostatic pressure measurement in the T, T^*, and T' compounds,[22] which confirms that the observed trends are not accidental due to a variety of materials but intrinsic within the CuO_2 plane. In contrast, the behavior of the bending mode frequency $\omega_{TO}(3)$, which is insensitive to the lattice constant a, can be understood in the framework of the usual lattice dynamics, considering the small change in a (from 3.81 to 4.00 Å) among the investigated materials.

The increase of dynamical contribution with increasing a, which causes the increase of e_T^* as in Eq. (5), gives rise also to the reduction of TO-phonon frequency. Adding the classical dipole field correction,[23] TO-phonon frequency is renormalized for bindary semiconductors as follows:[21]

$$\omega_{TO}^2 = \omega_0^2 \Omega_{DD}^2 - \frac{n}{Ma} \frac{\Xi^2}{E_G} . \tag{6}$$

The mechanical frequency ω_0 is related to the elastic property of material and is proportional to $a^{-3/2}$. The second term represents the reduction of phonon frequency due to the dipole-dipole interaction for the localized charge, while the last term gives the contribution from the electronic system.

When we compare $\omega_{TO}(4)$ among the transition metal oxides, La_2MO_4, a relatively small value of $\omega_{TO}(4)$ for $LaSrFeO_4$ can be understood as larger Ω_{DD} due to the large Z_0 value. In the case of cuprates, the contribution of the second term is not large and insensitive to a, as expected from the Z_0 value in Table IV. Therefore, the remarkable decrease of ω_{TO} with increasing a must come from the third term.

Generally, as predicted by the band theory, the deformation potential of the stretching type distortion is large in the perovskite related structure.[24] On the other hand, in the copper oxides, the electron correlation energy U (~ 6 eV) is larger than the charge transfer (CT) energy Δ (2 eV) which is the energy difference between O $2p$ and Cu $3d_{x^2-y^2}$ level. This means that these cuprates are not Mott insulators but CT insulators. The value of Δ can be experimentally determined by the optical absorption spectrum in the infrared and visible region. If CT energy is assumed to stand for E_G in Eqs. (5) and (6), the decrease of Δ also leads to the increase of dynamical term. In fact, a clear difference in Δ among the (2:1:4) compounds with T, T^*, and T' structure was reported by Tokura *et al.*[25] (2.0 eV for T structure with $a = 3.81$ Å, 1.8 eV for T^* structure with $a = 3.86$ Å, and 1.5 eV for T' structure with $a = 3.94$ Å.) Furthermore, quite recently, remarkable decrease of Δ with increasing a (a^{-7}) has been observed among the T' compounds with various lanthanide atoms.[22] Therefore, the change of Δ is supposed to be one of the origins for the change of ω_{TO}. The modulation of Cu-O bond distance (just corresponding to the Cu-O stretching phonon mode) would induce the modulation of Cu-O hybridization, which results in the modulation of charge transfer energy, and reversely the change of Δ would directly affect on the frequency of stretching mode phonon.

V. CONCLUSION

The optical phonon spectra for the single crystals of various layered cuprates as well as the isostructural noncopper oxides have been investigated. For T and T' compounds, the spectral anisotropy ($\mathbf{E} \perp \mathbf{c}$ and $\mathbf{E} \parallel \mathbf{c}$) was also successfully measured. By systematic study of comparison of the spectra among various compounds, almost all the phonon modes were unambiguously assigned, which are classified into the following common types: (i) two CuO_2 in-plane modes (stretching and bending type one), (ii) external mode, (iii) out-of-plane oxygen mode. For most of the phonon modes the difference of the phonon frequencies among the investigated materials can be understood in terms of the reduced mass difference among them, whereas the frequency of the in-plane stretching mode with nearly the same reduced mass for all of the materials was found to show strong dependence on the Cu-O bond distance.

The measurement for the single crystals enabled us to analyze the spectra quantitatively. As a result we could estimate various effective charges for each material. The extended effective charge of oxygen $|Z_0|e$ was small ($\sim 1.0e$) for all of the cuprates, which indicates the highly covalent character of these materials.

The small value of Z_0 implies that a large amount of e_T^* for the stretching mode is contributed from the electronic system. The strong a dependence of e_T^* as well as of ω_{TO} for the in-plane Cu-O stretching mode indicates the drastic change in the electronic system against a. The most dominant change in the electronic system induced by the change of Cu-O distance is the change of CT energy, which is evidenced by the remarkable decrease of Δ with increasing a observed in the T' (2:1:4) compounds. This change of Δ directly affects on the electron-phonon coupling, which results in the change of Cu-O stretching mode frequency. Therefore, the a dependence of large negative power for the stretching mode frequency just reflects the characteristic hybridization effect on the electronic system in the Cu oxides through the direct coupling of Cu-O bond modulation phonon with the CT excitation.

ACKNOWLEDGMENTS

The authors would like to thank Dr. Y. Tokura and Dr. N. Nagosa at the University of Tokyo for useful discussions about the electron-phonon interaction in the cuprate system.

---

[1] J. B. Torrance and R. M. Metzger, Phys. Rev. Lett. **63**, 1515 (1989); J. Kondo, Y. Asai, and S. Nagai, J. Phys. Soc. Jpn. **57**, 4334 (1988).

[2] The upper bound of T_c for the phonon-mediated superconductivity is predicted to be about 30 K by W. Weber, Phys. Rev. Lett. **58**, 1371 (1987).

[3] B. Renker, F. Compf, E. Gerig, N. Nucker, D. Ewert, W. Reichardt, and R. Rietschel, Phys. Rev. B **67**, 15 (1987).

[4] C. Taliani, R. Zamboni, G. Ruani, F. C. Matacotta, and K. I. Pokhodnya, Solid State Commun. **66**, 487 (1988).

[5] S. L. Cooper *et al.*, Phys. Rev. B **37**, 5920 (1988); R. Feile, U. Schmitt, P. Leiderer, J. Schubert, and U. Poppe, Z. Phys. B **72**, 161 (1988); S. Sugai, S. Shamoto, and M. Sato, Phys. Rev. B **38**, 6436 (1988).

[6] For example, the review article by R. Feile, Physica C **159**, 1 (1989).

[7] R. T. Collins, Z. Schlesinger, G. V. Chandrashekhar, and M. W. Shafer, Phys. Rev. B **39**, 2251 (1989).

[8] M. K. Crawford, G. Burns, and F. Holtzberg, Solid State Commun. **70**, 557 (1989).

[9] M. K. Crawford, G. Burns, G. V. Chandrashekhar, F. H. Dacol, W. E. Farneth, E. M. McCarron, III, and R. J. Smalley, Solid State Commun. **73**, 507 (1990).

[10] P. C. Eklund, A. M. Rao, G. W. Lehman, G. L. Doll, M. S. Dresselhaus, P. J. Picone, D. R. Gabbe, H. P. Jenssen, and G. Dresselhaus, J. Opt. Soc. Am. B **6**, 389 (1989).

[11] L. Pintshovius, J. M. Bassat, P. Odier, F. Gervais, G. Chervier, W. Reichardt, and F. Gompfp, Phys. Rev. B **40**, 2229 (1989).

[12] J.-M. Bassat, P. Odier, and F. Gervais, Phys. Rev. B **35**, 7126 (1987); F. Gervais, P. Echegut, J. M. Bassat and P. Odier, *ibid.* **37**, 9364 (1988).

[13] S. Tajima, S. Tanaka, T. Ido, and S. Uchida, in *Advances in Superconductivity II,* Proceedings of the 2nd International Symposium on Superconductivity, Tsukuba, 1989, edited by T. Ishiguro and K. Kajimura (Springer-Verlag, Heidelburg, 1990); S. L. Cooper, G. A. Thomas, J. Orenstein, D. H. Rapkine, M. Cappizi, T. Timusk, A. J. Millis, L. F. Schneemeyer, and J. V. Waszcak, Phys. Rev. B **40**, 11358 (1989); I. Terasaki, T. Nakahashi, S. Takebayashi, A. Maeda, and K. Uchinokura, Physica C **165**, 152 (1990).

[14] S. Tajima, S. Uchida, S. Ishibashi, T. Ido, H. Takagi, T. Arima, and Y. Tokura, Physica C **168**, 117 (1990).

[15] K. Sreedhar and P. Ganguley, Phys. Rev. B **41**, 371 (1990).

[16] J. F. Scott, Phys. Rev. B **4**, 1360 (1971).

[17] F. Gervais, Solid State Commun. **18**, 191 (1976).

[18] S. Uchida, S. Tajima, A. Masaki, S. Sugai, K. Kitazawa, and S. Tanaka, J. Phys. Soc. Jpn. **54**, 4395 (1985).

[19] S. Tajima, A. Masaki, S. Uchida, T. Matsuura, K. Fueki, and S. Sugai, J. Phys. C **20**, 3469 (1987).

[20] S. Tajima, H. Ishii, T. Nakahashi, T. Takagi, S. Uchida, M. Seki, S. Suga, Y. Hidaka, M. Suzuki, T. Murakami, K. Oka and H. Unoki, J. Opt. Soc. Am. B **6**, 475 (1989).

[21] S. Katayama and H. Kawamura, Solid State Commun. **21**, 521 (1977).

[22] T. Arima and Y. Tokura (unpublished).

[23] E. Burstein, A. Pinczuk, and R. F. Wallis, *The Physics of Semimetals and Narrow Gap Semiconductors* (Pergamon, New York, 1970).

[24] L. F. Mattheiss and D. R. Hamann, Phys. Rev. B **26**, 2686 (1982).

[25] Y. Tokura, S. Koshihara, T. Arima, H. Takagi, S. Ishibashi, T. Ido, and S. Uchida, Phys. Rev. B **41**, 11 657 (1990).

[26] J. Zaanen, G. A. Sawatzky, and J. W. Allen, Phys. Rev. Lett. **55**, 418 (1985).